Iminohydantoin Lesion Induced in DNA by Peracids and Other Epoxidizing Oxidants

ARTICLE *in* JOURNAL OF THE AMERICAN CHEMICAL SOCIETY · MAY 2009

Impact Factor: 12.11 · DOI: 10.1021/ja8090752 · Source: PubMed

J|A|C|S
ARTICLES

Published on Web 04/08/2009

Iminohydantoin Lesion Induced in DNA by Peracids and Other Epoxidizing Oxidants

Wenjie Ye,[†] R. Sangaiah,[†,‡] Diana E. Degen,[†] Avram Gold,[*,†] K. Jayaraj,[†] Karl M. Koshlap,[§] Gunnar Boysen,[†] Jason Williams,[||] Kenneth B. Tomer,[||] Viorel Mocanu,[‡,⊥] Nedyalka Dicheva,[⊥] Carol E. Parker,[⊥] Roel M. Schaaper,[#] and Louise M. Ball[†]

Department of Environmental Sciences and Engineering, CB7431, School of Pharmacy, CB7360, and UNC-Duke Proteomics Center, Program in Molecular Biology and Biotechnology, The University of North Carolina at Chapel Hill, Chapel Hill, North Carolina 27599, and Laboratories of Structural Biology, MD F0-03, and of Molecular Genetics, MD E3-01, National Institute of Environmental Health Sciences, National Institutes of Health, P.O. Box 12233, Research Triangle Park, North Carolina 27709

Received November 19, 2008; E-mail: golda@email.unc.edu

Abstract: The oxidation of guanine to 5-carboxamido-5-formamido-2-iminohydantoin (2-Ih) is shown to be a major transformation in the oxidation of the single-stranded DNA 5-mer d(TTGTT) by *m*-chloroperbenzoic acid (*m*-CPBA) and dimethyldioxirane (DMDO) as a model for peracid oxidants and in the oxidation of the 5-base pair duplex d[(TTGTT)·(AACAA)] with DMDO. 2-Ih has not been reported as an oxidative lesion at the level of single/double-stranded DNA or at the nucleoside/nucleotide level. The lesion is stable to DNA digestion and chromatographic purification, suggesting that 2-Ih may be a stable biomarker in vivo. The oxidation products have been structurally characterized and the reaction mechanism has been probed by oxidation of the monomeric species dGuo, dGMP, and dGTP. DMDO selectively oxidizes the guanine moiety of dGuo, dGMP, and dGTP to 2-Ih, and both peracetic and *m*-chloroperbenzoic acids exhibit the same selectivity. The presence of the glycosidic bond results in the stereoselective induction of an asymmetric center at the spiro carbon to give a mixture of diastereomers, with each diastereomer in equilibrium with a minor conformer through rotation about the formamido C−N bond. Labeling studies with [$^{18}O_2$]-*m*-CPBA and $H_2{}^{18}O$ to determine the source of the added oxygen atoms have established initial epoxidation of the guanine 4−5 bond with pyrimidine ring contraction by an acyl 1,2-migration of guanine carbonyl C6 to form a transient dehydrodeoxyspiroiminodihydantoin followed by hydrolytic ring-opening of the imidazolone ring. Consistent with the proposed mechanism, no 8-oxoguanine was detected as a product of the oxidations of the oligonucleotides or monomeric species mediated by DMDO or the peracids. The 2-Ih base thus appears to be a pathway-specific lesion generated by peracids and possibly other epoxidizing agents and holds promise as a potential biomarker.

Introduction

Aging, cancer, and degenerative diseases have been linked to DNA damage by reactive oxygen species.[1] Processes initiated by one-electron oxidations mediated by hydroxyl radical, ionizing radiation, and transition metals have been extensively characterized,[2−4] resulting in identification of numerous products from the oxidation of guanine, the most easily oxidized of the nucleobases. Of these, only 8-oxo-7,8-dihydroguanine (8-oxo-Gua), spiroiminohydantoin (Sp), and the guanine- and adenine-derived formamidopyrimidines (FapyG and FapyA) have been reported in vivo. 8-Oxo-Gua, found in vivo at background levels of $(1-2) \times 10^{-6}$ guanine,[5] is widely used as a biomarker of oxidative stress although it is not highly mutagenic.[3] By contrast, DNA damage by initial two-electron processes, whether direct or via rapid sequential one-electron oxidations, has only recently come into focus.[3−11] Our laboratory is examining oxidation of

[†] Department of Environmental Sciences and Engineering, The University of North Carolina at Chapel Hill.
[‡] Deceased.
[§] School of Pharmacy, The University of North Carolina at Chapel Hill.
[||] Laboratory of Structural Biology, National Institute of Environmental Health Sciences, National Institutes of Health.
[⊥] UNC-Duke Proteomics Center, Program in Molecular Biology and Biotechnology, The University of North Carolina at Chapel Hill.
[#] Laboratory of Molecular Genetics, National Institute of Environmental Health Sciences, National Institutes of Health.

(1) Klaunig, J. E.; Kamendulis, L. M. *Annu. Rev. Pharmacol. Toxicol.* **2004**, *44*, 239–267.
(2) Burrows, C. J.; Muller, J. G. *Chem. Rev.* **1998**, *98*, 1109–1151.
(3) Neeley, W. L.; Essigmann, J. M. *Chem. Res. Toxicol.* **2006**, *19*, 491–505.
(4) Dedon, P. C. *Chem. Res. Toxicol.* **2008**, *21*, 206–219.
(5) Gedick, C. M.; Boyle, S. P.; Wood, S. G.; Vaughan, N. J.; Collins, A. R. *Carcinogenesis* **2002**, *23*, 1441–1446.
(6) Hong, I. S.; Carter, K. N.; Sato, K.; Greenberg, M. M. *J. Am. Chem. Soc.* **2007**, *129*, 4089–4098.
(7) Kodama, T.; Greenberg, M. M. *J. Org. Chem.* **2005**, *70*, 9916–9924.
(8) Greenberg, M. M. *Org. Biomol. Chem.* **2007**, *5*, 18–30.
(9) Bellon, S.; Ravanat, J.-L.; Gasparutto, D.; Cadet, J. *Chem. Res. Toxicol.* **2002**, *15*, 598–606.
(10) Pratviel, G.; Meunier, B. *Chem.—Eur. J.* **2006**, *12*, 6018–6030.

10.1021/ja8090752 CCC: $40.75

Chart 1

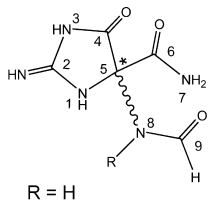

1, R = H
2a,b, R = ß-D-2-deoxyribofuranosyl
3a,b, R = ß-D-2-deoxyribofuranosyl-5-phosphate
4a,b, R = ß-D-2-deoxyribofuranosyl-5-triphosphate

DNA by peracids and by dimethyldioxirane (DMDO) as a model congruent in mechanism to peracids.[12,13] These compounds function as monooxygen donors by formally concerted, two-electron oxidations. Peracids may arise biologically during lipid peroxidation, through formation of triplet excited ketones and aldehydes by the Russell mechanism[14] followed by α-cleavage and coupling with O_2, by peroxidase-catalyzed autoxidation of aldehydes,[15] or by aldehyde oxidation catalyzed by transition metals.[16] In mitochondria, oxygenase activity of 2-oxoacid decarboxylases has been shown to generate high levels of peracids under certain conditions,[17,18] an observation that is significant because mitochondrial DNA repair capability appears to decrease with age[19,20] and accumulated mutations are implicated in age-related neuropathology and the aging process in general.[21]

Oxidation of guanine nucleobase by DMDO has been shown to yield exclusively 5-carboximado-5-formamido-2-iminohydantoin (2-Ih, **1**; see Chart 1),[22] a structure not previously reported as an oxidation product of guanine. The oxidation chemistry of guanine is complex, with multiple oxidation pathways possible, depending on the reaction conditions and steric environment. In deoxyguanosine both the glycosidic linkage and the deoxyribose moiety offer additional reactive sites, and in oligonucleotides and DNA, neighboring bases may alter reaction pathways by influencing accessibility. The action of *m*-chloroperbenzoic acid (*m*-CPBA) on DNA appears to be associated with damage targeted to purines that is strongly blocking to replication, particularly in loop regions.[23] Guanine is reported to be the predominant target of both peracids and DMDO,[15,23,24] but no information is available regarding the structural nature of the lesions. Alternative products of DMDO or *m*-CPBA oxidation of guanine in DNA could include formation of *N*-oxide, *N*-hydroxylamine, and nitro derivatives.[25,26] Thus, while oxidation of the nucleobase model can provide useful information about the structure and the mechanism of formation of 2-Ih, demonstration of the formation of 2-Ih at the nucleoside and DNA levels is a critical step in establishing biological significance of this lesion.

In this study, we report that DMDO generates 5-carboxamido-5-formamido-2-iminohydantoin from guanine in single- and double-stranded DNA sequences. These observations indicate that the presence of the glycosidic bond and flanking and partner bases in DNA does not redirect the oxidation toward different products and that 2-Ih may therefore be significant as a blocking lesion generated in vivo by peracids. We also report labeling studies with [$^{18}O_2$]-*m*-CPBA and $H_2{}^{18}O$ to identify the source of the added oxygens and have conclusively established the oxidation mechanism shown in Scheme 1. Consistent with Scheme 1, no 8-oxo-Gua was detected as a product of the oxidations mediated by DMDO or the peracids. 2-Ih thus appears to be a pathway-specific lesion and holds promise as a potential biomarker.

Experimental Procedures

Instrumentation. NMR spectra were recorded on a Varian Inova NMR spectrometer operating at 500 MHz for ^{1}H and at 125 MHz for ^{13}C. ^{13}C shifts were obtained from HSQC and HMBC spectra, and $^1J_{C-H}$ values were derived from unsuppressed one-bond coupling in the heteronuclear shift correlation spectra. Low-resolution electrospray ionization mass spectrometry (ESI-MS) and tandem mass spectrometry (ESI-MS/MS) were performed on a Finnigan DECA ion trap system. Liquid chromatography−ESI-MS (LC−ESI-MS) and LC−ESI-MS/MS were performed on a Finnigan TSQ Quantum system. Exact mass measurements were acquired on an IonSpec HiRes QFT ion cyclotron resonance mass spectrometer (Lake Forest, CA) equipped with a 9.4 T superconducting magnet and a Waters/Micromass Z-spray source. Samples were injected at a flow rate of 500 nL/min. The instrument was employed in the positive ion and broad-band modes with a probe voltage of 3.2 kV, a cone voltage of 45 V, an accumulation in Q3 of 5000 ms, and the quadrupole ion guide burst optimized to transmit ions in the 200 *m*/*z* mass range. Matrix-assisted laser desorption/ionization MS (MALDI-MS) data were acquired on a Bruker Ultraflex II MALDI-time-of-flight (TOF)/TOF mass spectrometer (Bruker Daltonics, Billerica, MA). Samples were dissolved in 50/50 MeOH/0.1% TFA, and MALDI spectra were acquired in the negative ion reflectron mode, using α-cyano-4-hydroxycinnamic acid as the matrix. Spectra were acquired over the mass range 500−2500 Da, using ACTH(1−17) and ACTH(18−39) as calibration standards.

Chemicals. dGuo, dGMP, dGTP, 77% *m*-CPBA, and 32% peracetic acid purchased from Sigma-Aldrich (Milwaukee, WI) were used as received. DMDO was generated by potassium monopersulfate oxidation of acetone and was analyzed by iodometric titration immediately prior to use.[26] d(TTGTT) and d(AACAA) were synthesized by the Oligonucleotide Synthesis Core Facility at The University of North Carolina at Chapel Hill and purified by HPLC on a reversed-phase Vydac C18 250 × 4.6 mm column eluted with a linear gradient of 8−15% MeOH in water over 10 min at a flow rate of 1 mL/min monitored at a detector wavelength of 260 nm.

[$^{18}O_2$]-*m*-CPBA was synthesized as follows (T. G. Spiro, personal communication). A flask containing methylene chloride (35 mL) and *m*-chlorobenzaldehyde (3 mL) was degassed by three

(11) Xu, X.; Muller, J. G.; Ye, Y.; Burrows, C. J. *J. Am. Chem. Soc.* **2008**, *130*, 703–709.
(12) Bach, R. D.; Dmitrenko, O.; Adam, W.; Schambony, S. *J. Am. Chem. Soc.* **2003**, *125*, 924–934.
(13) Porter, N. A.; Yin, H.; Pratt, D. A. *J. Am. Chem. Soc.* **2000**, *122*, 11272–11273.
(14) Russell, G. *J. Am. Chem. Soc.* **1957**, *79*, 3871–3877.
(15) Adam, W.; Kurz, A.; Saha-Möller, C. R. *Free Radical Biol. Med.* **1999**, *26*, 566–579.
(16) Nam, W.; Kim, H.; Hoon, J. S.; Raymond, K.; Ho, Y. N.; Valentine, J. S. *Inorg. Chem.* **1996**, *35*, 1045–1049.
(17) Abell, L. M.; Schloss, J. V. *Biochemistry* **1991**, *30*, 7883–7887.
(18) Bunik, V. I.; Schloss, J. V.; Pinto, J. T.; Gibson, G. E.; Cooper, A. J. L. *Neurochem. Res.* **2007**, *32*, 871–891.
(19) Ledoux, S. P.; Druzhyna, N. M.; Hollensworth, S. B.; Harrison, J. F.; Wilson, G. L. *Neuroscience* **2007**, *145*, 1249–1259.
(20) Croteau, D. L.; Stierum, R. H.; Bohr, V. A. *Mutat. Res.* **1999**, *434*, 137–148.
(21) Dimauro, S.; Davidzon, G. *Ann. Med.* **2005**, *37*, 222–232.
(22) Ye, W.; Sangaiah, R.; Degen, D. E.; Gold, A.; Jayaraj, K.; Koshlap, K. M.; Boysen, G.; Williams, J.; Tomer, K. B.; Ball, L. M. *Chem. Res. Toxicol.* **2006**, *19*, 506–510.
(23) Jacobsen, J. S.; Humayun, M. Z. *Carcinogenesis* **1986**, *7*, 491–493.
(24) Davies, J. R.; Boyd, D. R.; Kumar, S.; Sharma, N. D.; Stevenson, C. *Biochem. Biophys. Res. Commun.* **1990**, *169*, 87–94.
(25) Begtrup, M.; Verdsø, P. *J. Chem. Soc., Perkin Trans. 1* **1995**, 243–247.
(26) Murray, R. W. *Chem. Rev.* **1989**, *89*, 1187–1201.

Scheme 1

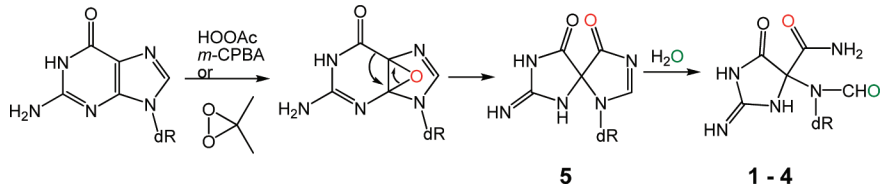

5 1 - 4

freeze−thaw cycles on a high-vacuum manifold and frozen in liquid nitrogen under vacuum (1×10^{-3} mm), and then $^{18}O_2$ (500 mL, >95%) from a break-seal vessel was condensed into the reaction flask. The reaction flask was isolated, removed from the vacuum line, and irradiated with a Fisher Biotech UV lamp at 365 nm with vigorous stirring for 8 h at −20 °C. Following transfer to a round-bottom flask, the reaction mixture was reduced in volume under aspirator pressure to 10 mL and the precipitate collected by filtration and washed with cold hexane, yielding 700 mg of [$^{18}O_2$]-*m*-CPBA, activity 55% by iodometric titration.

Oxidation of d(TTGTT) by DMDO. d(TTGTT) (1 μmol) in 0.5 mL of 0.1 M $NaHCO_3$ buffer (pH 8.1) was cooled in an ice bath and treated with 80 μL of 0.09 M DMDO in acetone for 30 min, and the total reaction mixture was then lyophilized. The total crude reaction mixture was analyzed by MALDI-TOF and positive and negative ion ESI-MS. The reaction mixture was then separated by HPLC on a Vydac C18 250 × 2.1 mm, 5 μm column eluted with 0−10% MeOH in 10 mM TEAA over 20 min at a flow rate of 1 mL/min and showed one major peak at 9.5 min. ESI-MS data on the collected peak were acquired by loop injection under the following conditions: 25% methanol/75% 10 μM aqueous ammonium formate (pH 6.0) at an injector flow rate of 50 μL/min.

Digestion of Oxidized d(TTGTT). d(TTGTT) (2 μmol) was oxidized as described above. An aliquot of the crude reaction mixture (∼400 nmol) was dissolved in 1050 μL of a solution of 20 mM $MgCl_2$ in 80 μM Tris−HCl buffer (pH 7.4) to which 50 μL of DNase I (bovine pancreas, 4000 U/mL) was added. Doubly distilled water was added to bring the total volume to 2100 μL, and the sample was vortexed and incubated at 37 °C for 10 min. Alkaline phosphatase (50 μL, type VII-T, from bovine intestinal mucosa, 200 U/mL) and phosphodiesterase I (50 μL, type II, from *Crotalus ademanteus* venom, 0.26 U/mL) were added, and the sample was vortexed and incubated at 37 ° for 60 min. Protein was removed by Centricon-10 filtration for 90 min at 4 °C, and the filters were rinsed by addition of H_2O followed by centrifugation for a further 90 min. The combined filtrates were lyophilized, and the product was separated by HPLC on an Econosphere C8 column (9.4 × 250 mm) eluted at 2 mL/min using a gradient of 5−40% MeOH in water over 30 min.

Oxidation of d(TTGTT) by *m*-CPBA. To d(TTGTT) (3.8 mg, 2.29 μmol) dissolved in 5 mL of 0.1 mM ammonium acetate buffer at pH 4.65 was added dropwise with stirring 0.5 mL of a methanol solution of *m*-CPBA (5.1 mg, 22.9 μmol). After 48 h, the reaction mixture was extracted with 3 × 5 mL of dichloromethane. The aqueous portion was lyophilized and the residue analyzed by ESI-MS/MS following desalting by ZIPTIP C_{18} (Millipore Corp., Billerica, MA).

Oxidation of d[(TTGTT)·(AACAA)]. A 0.9 μmol portion of d(TTGTT) in 465 μL of 50 mM NaCl and 0.1 M $NaHCO_3$ (pH 6.5) was mixed with 1 μmol of d(AACAA) (11% molar excess) in 500 μL of 50 mM NaCl and 0.1 M $NaHCO_3$ (pH 6.5), and the resulting mixture was heated to 90 °C and slowly cooled to 0 °C [the calculated T_m of the duplex under the oxidation conditions was 20 °C[27]]. The duplex was oxidized and digested as described above. The mixture obtained from lyophilization of the Centricon-10 filtrates was separated on an Econosphere C8 column (9.4 × 250 mm) eluted at 2 mL/min using a gradient of 0−30% MeOH in water over 20 min.

(27) Kibbe, W. A. *Nucleic Acids Res.* **2007**, *35*, W43 (Web server issue).

Oxidation of dGuo by Peracetic Acid. A solution of 0.1 mmol of dGuo and 50 μL of 32% peracetic acid (0.2 mmol) in 10 mL of H_2O was stirred at ambient temperature, with further additions of 0.2 mmol of peracetic acid at 24, 48, and 68 h. Ammonium carbonate (27 mg) was added during the reaction to maintain a pH of ∼3.9. After 72 h, most of the volatiles were removed under a stream of Ar, and the residue was lyophilized overnight. The resulting solid residue was separated by semipreparative HPLC on an Econosphere C8 column (9.4 × 250 mm) eluted isocratically at 2 mL/min with 13% methanol in deionized water. Peaks at 6.4 min (spiroiminodihydantoin nucleoside, Sp-dR), 6.6 min (spiroiminodihydantoin base, Sp), 7 min (2-Ih), and 15.8 min (dGuo) were collected and characterized by NMR and ESI-MS. A yield of 25% 2-Ih was estimated from the chromatographic trace at 230 nm by comparing the peak areas (adjusted for ε_{230}), 2-Ih/(Sp-dR + Sp + 2-Ih + dGuo).

Oxidation of dGuo by *m*-CPBA. dGuo (0.1 mmol) and 0.1 mmol of *m*-CPBA in 10 mL of 9/1 aqueous buffer (0.1 M NH_4OAc, pH 4.5)/methanol were stirred at ambient temperature with a further addition of 0.1 mmol of *m*-CPBA at 36 h. After 72 h, *m*-CBA and residual *m*-CPBA were extracted with 3 × 5 mL of CH_2Cl_2, and the aqueous reaction layer was lyophilized overnight. The resulting residue was separated by semipreparative HPLC on an Econosphere C8 column (9.4 × 250 mm) eluted isocratically at 2 mL/min with 10% methanol in deionized water. Peaks at 7 min (2-Ih-dR/2-Ih, 3/1, 80% resolved) and 15.8 min (dGuo) were collected. A combined yield of 79% 2-Ih-dR + 2-Ih was determined from the chromatographic trace at 230 nm by comparing the peak areas (adjusted for ε_{230}), (2-Ih-dR + 2-Ih)/(2-Ih-dR + 2-Ih + dGuo).

Oxidation of dGuo by [$^{18}O_2$]-*m*-CPBA. Oxidation of dGuo with [$^{18}O_2$]-*m*-CPBA was performed as described above, except that [$^{18}O_2$]-*m*-CPBA was used in place of natural abundance *m*-CPBA.

Incorporation of ^{18}O into 2-Ih from $H_2{}^{18}O$. Gua (0.001 mmol) was suspended in 0.2 mL of H_2O and dissolved by slow addition of 0.2 mL of 1% (w/v) aqueous NaOH. Then 0.4 mL of $H_2{}^{18}O$ was added, the reaction mixture was cooled in an ice bath, and 0.15 mL of 0.1 M DMDO in acetone was added. After the mixture was stirred for 30 min, the solvents were evaporated under a stream of Ar, and the solid was analyzed by ESI-MS.

Oxidation of dGuo by DMDO. dGuo (0.1 mmol) was dissolved in 10 mL of $NaHCO_3$ buffer (pH 8.1) cooled in an ice bath. To this solution was added with stirring DMDO in acetone (1.2 mL, 0.10 M), and after 30 min, acetone was evaporated under a stream of Ar. The remaining aqueous solution was lyophilized overnight to give a mixture of products and salts as an off-white powder. The diastereomers were desalted by semipreparative HPLC on an Econosphere C8 column (9.4 × 250 mm) eluted isocratically with 30% MeOH in water at 2 mL/min, and the product mixture was collected as a single peak at a retention time of ∼8.25 min. UV: $\lambda_{max}(H_2O)$ 230 nm. Positive ion ESI-MS: *m/z* 302 ($[MH]^+$). Positive ion ESI-MS/MS on *m/z* 302 ($[MH]^+$): 284 ($[MH - H_2O]^+$), 186 ($[MH - deoxyribose]^+$), 141 ($[MH - deoxyribose - formamide]^+$). Positive ion high-resolution Fourier transform ICR-ESI-MS (as protonated dimer): *m/z* calcd for $[C_{10}H_{15}N_5O_6]_2H^+$ 603.21229, found 603.21511. ^1H NMR (500 MHz, D_2O, 5 °C): **2a**, 8.59 (s, 1H, H9), 5.62 (ψt, 1H, $J = 7.06$ Hz, H1′), 4.35 (m, 1H, H3′), 3.93 (m, 1H, H4′), 3.82, 3.72, m, H5′, H5″ overlapping with other isomers), 2.61 (m, >1H, H2″, overlapping with H2″-**2b**), 2.31 (m, 1H, H2′) ppm; **2b**, 8.65 (s, 1H, H9), 5.57 (ψt, 1H, $J = 6.61$ Hz, H1′), 4.43 (m, 1H, H3′), 3.98 (m, 1H, H4′), 3.70−3.64 (m, H5′, H5″, overlapping

with other isomers), 2.61 (m, >1H, H2″, overlapping with H2″-**2a**), 2.45 (m, 1H, H2′) ppm; **2a′**, 8.36 (s, 1H, H9), 5.72 (m, 1H, H1′), 4.39 (m, 1H, H3′), 2.59 (m, 1H, H2″) ppm; **2b′**, 8.31 (s, 1H, H9), 5.68 (1H, H1′), 4.46 (m, 1H, H3′) ppm. ^{13}C NMR (125 MHz, D_2O, 5 °C): **2a**, 164.2 (C6), 163.8 ($^1J_{C9-H9}$ = 206.3 Hz, C9), 85.5 ($^1J_{C1'-H1'}$ = 170.4 Hz, C1′), 83.3 ($^1J_{C4'-H4'}$ = 148.0 Hz, H4′), 76.2 (C5), 67.8 ($^1J_{C3'-H3'}$ = 152.8 Hz, H3′), 58.9 (C5′), 37.2 ($^1J_{C2'-H2''}$ = 148.5 Hz, C2′) ppm; **2b**, 163.8 ($^1J_{C9-H9}$ = 207.0 Hz, C9), 85.2 ($^1J_{C1'-H1'}$ = 171.6 Hz, C1′), 84.1 ($^1J_{C4'-H4'}$ = 149.2 Hz, H4′), 76.7 (C5), 68.1 ($^1J_{C3'-H3'}$ = 152.3 Hz, H3′), 64.1 (C5′), 35.5 ($^1J_{C2'-H2''}$ = 138.4 Hz, C2′) ppm.

Separation of Diastereomers 2a and 2b. Diastereomers **2a** and **2b** from the oxidation of dGuo described above were separated by semipreparative HPLC on an AQUASIL C18 column (10 × 250 mm) eluted isocratically with 1.5% acetonitrile in 17 mM ammonium acetate. Peaks were collected at 8.84 min (**2b**) and 9.40 min (**2a**). Proton shifts of **2a** and **2b** observed in ^{1}H NMR, NOESY, and ROESY spectra (500 MHz, D_2O, 5 °C) were identical to those assigned to **2a** and **2b** in the mixture above.

Oxidation of dGMP by DMDO. dGMP (0.1mmol) was dissolved in 10 mL of 0.1 M $NaHCO_3$ buffer (pH 8.1) with stirring in an ice bath. To this solution was added with stirring 1.2 mL of 0.10 M DMDO in acetone. After 30 min, the acetone was evaporated under a stream of Ar and the residue lyophilized overnight to give an off-white powder. Desalting was accomplished by semipreparative HPLC on an Econosphere C8 column (9.4 × 250 mm) eluted isocratically with 30% MeOH in H_2O at 2 mL/min. The mixture of diastereomers was collected as a single peak, with a retention time of ~4.7 min. UV: $\lambda_{max}(H_2O)$ 230 nm. Negative ion ESI-MS: *m/z* 380 ([MH]$^-$). Negative ion ESI-MS/MS on *m/z* 380 ([MH]$^-$): 337 ([MH − formamide]$^-$), 240 ([MH − 5-formamido-2-iminohydatoin]$^-$). Positive ion high-resolution Fourier transform ICR-ESI-MS (as protonated dimer): *m/z* calcd for $[C_{10}H_{15}N_5O_6]_2H^+$ 763.14495, found 763.14832. ^{1}H NMR (500 MHz, D_2O, 5 °C): **3a**, 8.21 (s, 1H, H9), 5.70 (ψt, 1H, $J \approx 6.7$ Hz, H1′), 4.35 (m, 1H, H3′), 3.95 (m, 1H, H4′), 3.73−3.56 (m, overlapping with other isomers, H5′, H5″), 2.36 (m, 1H, H2″), 1.91 (m, 1H, H2′) ppm; **3b**, 8.50 (s, 1H, H9), 5.38 (ψt, 1H, $J \approx 5.5$ Hz, H1′), 4.39 (m, 1H, H3′), 3.79 (m, 1H, H4′), 3.73−3.56 (m, overlapping with other isomers, H5′, H5″), 2.55 (m, 1H, H2″), 2.20 (m, 1H, H2′) ppm; **3a′**, 8.38 (s, 1H, H9), 5.47 (ψt, 1H, $J \approx 5.4$ Hz, H1′), 4.27 (m, 1H, H3′), 3.83 (m, 1H, H4′), 3.73−3.56 (m, overlapping with other isomers, H5′, H5″), 2.41 (m, 1H, H2″), 2.17 (m, 1H, H2′) ppm; **3b′**, 8.32 (s, 1H, H9), 6.01 (dd, 1H, $J \approx 4.8$, 9.4 Hz, H1′), 4.31 (m, 1H, H3′), 3.88 (m, 1H, H4′), 3.73−3.56 (m, overlapping with other isomers, H5′, H5″) (H2″, H2′ not resolved) ppm. ^{13}C NMR (125 MHz, D_2O, 5 °C): **3a**, 180.5 (C4), 171.9 (C2), 167.1 (C6), 164.6 ($^1J_{C9-H9}$ = 206.9 Hz, C9), 88.3 (C1′), 87.7 ($^3J_{P-C4'}$ = 8.6 Hz, C4′), 79.0 (C5), 71.8 (C3′), 64.2 ($^3J_{P-C5'}$ = 4.5 Hz, C5′), 42.0 ($^1J_{C2'-H2''}$ = 136.8 Hz, C2′) ppm; **3b**, 181.9 (C4), 171.8 (C2), 167.3 (C6), 166.5 ($^1J_{C9-H9}$ = 207.9 Hz, C9), 88.7 (C1′), 86.3 ($^3J_{P-C4'}$ = 9.0 Hz, C4′), 79.6 (C5), 71.7 (C3′), 64.4 ($^3J_{P-C5'}$ = 4.2 Hz, C5′), 39.0 (C2′) ppm; **3a′**, 181.8 or 182.6 (C4), 172.1 (C2), 167.5 (C6), 165.6 ($^1J_{C9-H9}$ = 208.2 Hz, C9), 88.6 (C1′), 85.9 ($^3J_{P-C4'}$ = 8.7 Hz, C4′), 78.7 (C5), 71.5 (C3′), 65.3 ($^3J_{P-C5'}$ = 4.6 Hz, C5′) (C2′ not resolved) ppm; **3b′**, 182.4 (C4), 171.4 (C2), 163.8 (C9), 85.4 ($^3J_{P-C4'}$ = 7.9 Hz, C4′), 84.7 (C1′), 79.0 (C5), 72.3 (C3′) (C2′ and C5′ signals could not be resolved) ppm.

Oxidation of dGTP by DMDO. dGTP (0.05 mmol) was dissolved in 0.1 mM $NaHCO_3$ buffer (pH 8.1) at 0 °C. To this solution was added with stirring 0.75 mL of 0.081 M DMDO in acetone. After the resulting solution was stirred for 30 min at 0 °C, acetone was removed under a stream of Ar and the reaction mixture lyophilized and stored at −80 °C. The product mixture (**4**) was characterized without further purification. Negative ion ESI-MS: *m/z* 584 ([MNa$_2$ − H]$^-$), 562 ([MNa − H]$^-$), 540 ([M − H$^-$), 460 ([M − H_2PO_3]$^-$], 387 ([MNa − HP_2O_7]$^-$). ^{1}H NMR (500 MHz, D_2O, 0 °C): 8.45 (s), 8.43 (s), 8.42 (s), 8.18 (s), 5.90 (m), 5.75 (m), 5.59 (m), 4.51 (m), 4.48 (m), 4.36 (m), 4.24 (m), 4.16 (m), 4.04−3.83 (m), 2.60−2.44 (unresolved), 2.32 (m), 2.17 (m) ppm.

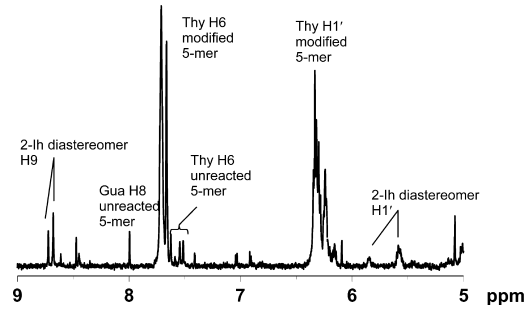

Figure 1. ^{1}H NMR (500 MHz, D_2O) spectrum of oxidized d(TTGTT) in the H1′−H9 range. Signals identified with 2-Ih are indicated on the trace.

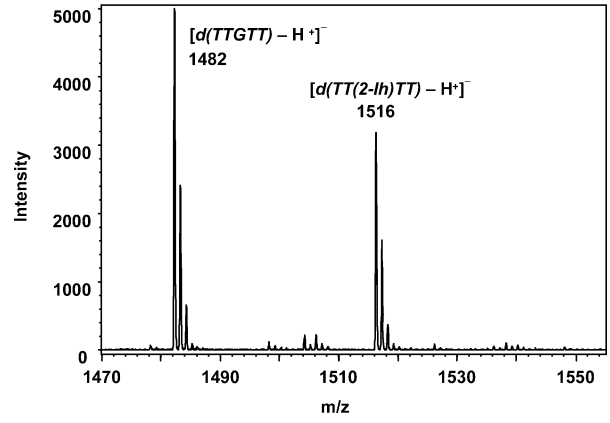

Figure 2. Negative ion MALDI-TOF mass spectrum of the total reaction mixture of oxidized d(TTGTT) showing the unoxidized 5-mer (*m/z* 1482) and product at +34 mass units (*m/z* 1516).

Results

Oxidation of d(TTGTT). Following treatment of the 5-mer with a 7-fold excess of DMDO, the total crude reaction mixture was analyzed directly by NMR, MALDI-TOF, and ESI-MS. In the ^{1}H NMR spectrum of the total reaction mixture (Figure 1), pairs of signals are present at 8.72/5.84 and 8.68/5.57 ppm with a 1/4 ratio. The resonances at 5.57 and 5.84 ppm are in the region associated with H1′ signals, while those at 8.68 and 8.72 ppm are singlets in the region where the formyl H9 of 2-Ih is expected (ref 24 and vide infra). The pattern observed in Figure 1 is consistent with formation of 2-Ih diastereomers in the oxidized 5-mer in a 1 to 4 ratio. On the basis of integrated signals from the unreacted 5-mer and the 2-Ih diastereomers, >95% of the 5-mer was oxidized, with at least 40% conversion to 2-Ih-containing product. The MALDI-TOF mass spectrum in the negative ion mode showed a strong ion at *m/z* 1516, corresponding to a gain of 34 mass units over the unmodified 5-mer as expected for formation of the 2-Ih lesion (Figure 2). The negative ion ESI-MS acquired by loop injection (Figure S1, Supporting Information) shows strong ions at *m/z* 1516 and 758 as expected for the [M − H]$^-$ and [M − H]$^{2-}$ ions, respectively, of the 5-mer containing the 2-Ih modification. In the ESI-MS spectrum, ions corresponding to unmodified 5-mer are not observed, consistent with the estimate from the NMR spectrum that only 5% of the 5-mer was unreacted and that a substantial proportion of the 5-mer was converted to the 2-Ih-modified oligonucleotide. ESI-MS/MS of the ion at *m/z* 1516

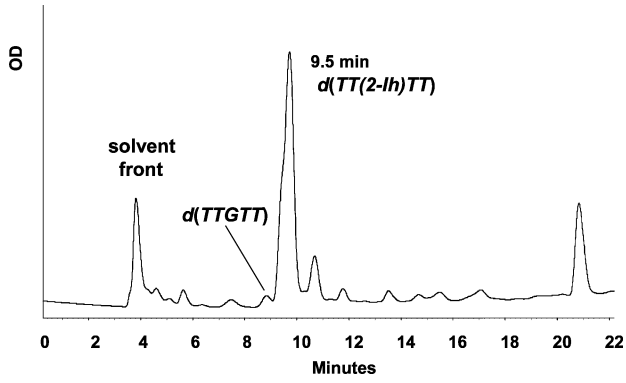

Figure 3. HPLC trace (detector at 260 nm) of the reaction mixture from DMDO oxidation of the 5-mer. Peaks at 10.7 and 20.8 min were not identifiable.

(Figure S2, Supporting Information) yielded a product ion at *m/z* 1376 corresponding to loss of a 2-iminoimidazole fragment (2-imino-5-oxo-2,5-dihydro-1*H*-4-imidazole-4-carboxamide) to yield a ribosyl formamide-containing 5-mer anion, a fragmentation pattern consistent with oxidation of the Gua to 2-Ih. The positive ion ESI-MS (Figure S3, Supporting Information) by loop injection was entirely in accord with this result, having ions at *m/z* 1518 ($[MH]^+$) and 1540 ($[MNa]^+$), along with product ions at *m/z* 1400 for loss of 2-iminoimidazole from $[MNa]^+$, 729 (sodium adduct of [5′-*O*-(2-methylene-2,3-dihydrofuran-3-yl)-pdTpdT]$^+$), 671 (disodium adduct of $[pdT]_2^+$), and 649 (sodium adduct of $[pdT]_2^+$) and no protonated molecular ion corresponding to the unmodified 5-mer. ESI-MS/MS of $[MH]^+$ (Figure S4, Supporting Information) yielded a product ion at *m/z* 1378 ($[MH]^+ - 2$-iminoimidazole). The HPLC trace of the reaction mixture showed a major peak at 9.5 min (Figure 3). In the positive ion ESI-MS spectrum of this collected peak, a major ion at *m/z* 1540 was identified as the sodium adduct $[MNa]^+$ of the 2-Ih-modified 5-mer by ESI-MS/MS, which gives a product ion at *m/z* 1400, corresponding to the sodium adduct of the 5-mer containing ribosylformamide following loss of the 2-iminoimidazole fragment (Figure S5, Supporting Information). The slight inflection at the leading edge of the 9.5 min peak in Figure 3 may represent the unoxidized 5-mer (5% by ^{1}H NMR, not detected in the ESI-MS spectrum of the collected peak) or partially resolved diastereomeric product. In the mixture of mononucleosides resulting from digestion of the oxidized 5-mer, 2-Ih-dR was definitively identified both by the HPLC retention time (vide infra) and by the protonated molecular ion (*m/z* 302) in the ESI-MS spectrum. These data establish transformation of guanine to 2-Ih as the major oxidation pathway of the 5-mer. Treatment of the 5-mer with *m*-CPBA yields a product mixture having an ion at *m/z* 1518 by positive ion ESI-MS, confirmed as 2-Ih by ESI-MS/MS, which yields the expected product ion at *m/z* 1378.

Oxidation of d[(TTGTT)·(AACAA)]. d(TTGTT) complexed to its complement d(AACAA) present in 11% excess was oxidized by DMDO under the same conditions as the single-stranded 5-mer, and the reaction mixture was digested to nucleosides. The presence of 2-Ih-dR in the digest was confirmed by the retention time and ESI-MS/MS of the collected peak (Figure S6, Supporting Information).

Oxidation of dGuo by Peracids. Figure 4 shows the HPLC traces of reaction mixtures from peracetic acid and *m*-CPBA oxidations of dGuo. 2-Ih aglycon, Sp aglycon, and Sp-dR were identified by ESI-MS and chromatographic retention times in the peracetic acid oxidation. The yields of 2-Ih and total spiroiminodihydantoins (aglycon + nucleoside) were estimated to be ~25% and 50%, respectively, from integration of the HPLC peaks in Figure 4a adjusted for extinction coefficients, assuming approximately equivalent extinction coefficients for the broad absorption maximum of the three oxidation products at 230 nm. Oxidation of dGuo by *m*-CPBA gave 2-Ih and 2-Ih-dR in a combined yield of 79%, and Figure 4b shows that they are the only products present in significant yield. The mass spectrum of the broad, low peak eluting at 4 min (Figure 4b) shows traces of *m*-chlorobenzoic acid and Sp/Sp-dR. At an estimated limit of detection of 1% of the total yield of oxidation products, no 8-oxo-dGuo was found in the HPLC and ESI-MS analysis of the peracid oxidation mixtures.

^{18}O Labeling Reactions. We addressed the origins of the incorporated oxygen atoms in two experiments: (1) by oxidizing guanine with DMDO in 1/1 $H_2{}^{18}O/H_2O$ and (2) by oxidizing deoxyguanosine with $[^{18}O_2]$-*m*-CPBA (>95% $^{18}O_2$). The use of deoxyguanosine for oxidation with $[^{18}O_2]$-*m*-CPBA was dictated by the insolubility of guanine in aqueous medium at pH 4.5 required for activity of this peracid. Negative ion ESI-MS analysis of the oxidation mixture obtained with DMDO in 1/1 $H_2O/H_2{}^{18}O$ yielded the mass spectrum shown in Figure 5a in which the [^{18}O]-2-Ih isotopomer is >40% of the natural abundance 2-Ih isotopomer. Making allowances for contamination of the reaction with natural abundance water from the acetone solution of DMDO and from atmospheric condensation during transfer of the cold (−80 °C) DMDO, the $^{16}O/^{18}O$ ratio in the product is in accord with incorporation of 50% of one atom of ^{18}O. Comparison of the negative ion ESI-MS/MS spectra of the $[M - H]^-$ ions of the labeled and unlabeled 2-Ih shows that ^{18}O is lost with the formamide fragment (Figure 5b,c).

Exchange of the formamido oxygen with $H_2{}^{18}O$ during workup was ruled out by determining that no ^{18}O incorporation could be detected on stirring natural abundance 2-Ih in $H_2{}^{18}O$ under the reaction conditions for 2 h. In the positive ion ESI-MS spectrum of the product from oxidation of dGuo with $[^{18}O_2]$-*m*-CPBA, the protonated molecular ion shifts from *m/z* 302 to *m/z* 304, indicating complete incorporation of a single ^{18}O label. The major product ions in the positive ion ESI-MS/MS spectrum (Figure 6) of the ion at *m/z* 304 corresponded to loss of the deoxyribose (*m/z* 188), loss of deoxyribose along with natural abundance CO (*m/z* 160), and loss of natural abundance deoxyribosylformamide (*m/z* 143). As shown in Figure 6, ^{18}O label is retained in the product ions corresponding to loss of deoxyribose, CO, and deoxyribosylformamide.

Oxidation of dGuo by DMDO. Product from desalting the DMDO oxidation mixture by semipreparative HPLC was collected as a single peak which, by accurate mass measurement, corresponded in composition to the protonated dimer $(2\text{-Ih-dR})_2H^+$. ESI-MS/MS of the protonated molecule (MH^+) yielded the same product ions as shown in Figure 6a for 2-Ih-dR from oxidation of dGuo by natural abundance *m*-CPBA. Multiple signals in the ^{1}H NMR spectrum of the total reaction mixture (Figure 7) were identified at chemical shifts expected for formyl H9[22] of the 2-Ih base and H1′ of the deoxyribose,[28] indicating the presence of diastereomers. In all, the reaction mixture appeared to contain two major and two minor species. The

(28) Ippel, J. H.; Wijmenga, S. S.; de Jong, R.; Heus, H. A.; Hilbers, C. W.; de Vroom, E.; van der Marel, G. A.; van Boom, J. H. *Magn. Reson. Chem.* **1996**, *34*, S156–Sl76.

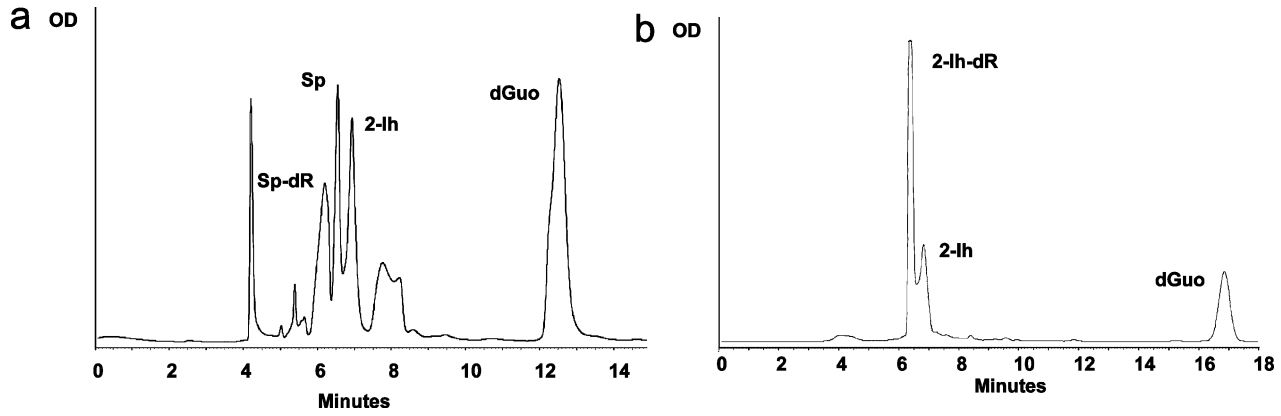

Figure 4. HPLC traces (detector set at 230 nm) of reaction mixtures from dGuo oxidation by (a) peracetic acid and (b) *m*-CPBA, following extraction of spent oxidant. Products identified are indicated on the traces.

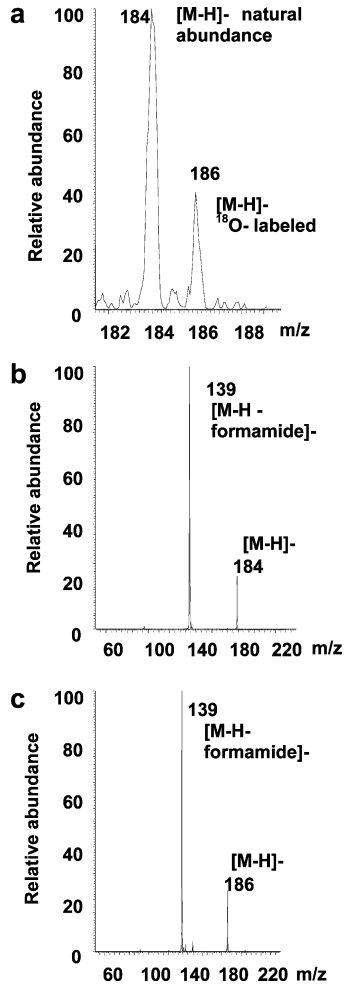

Figure 5. (a) Negative ion ESI-MS spectrum showing the $^{16}O/^{18}O$ distribution in 2-Ih base from DMDO oxidation of Gua in a 1/1 mixture of $H_2{}^{16}O/H_2{}^{18}O$. (b) Negative ion ESI-MS/MS spectrum of the molecular ion of natural abundance 2-Ih. (c) Negative ion ESI-MS/MS spectrum of molecular ion ^{18}O-labeled 2-Ih showing loss of the label with the formamide moiety.

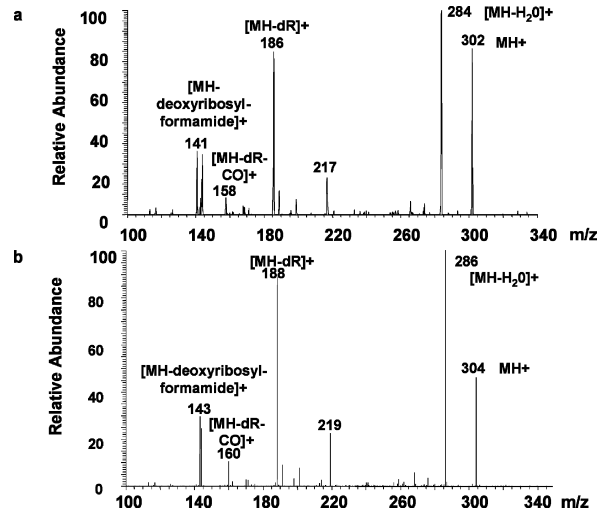

Figure 6. Positive ion ESI-MS spectrum of 2-Ih-dR from oxidation of dGuo with (a) natural abundance *m*-CPBA and (b) [$^{18}O_2$]-*m*-CPBA, indicating retention of ^{18}O label in the product ion at *m/z* 143 from loss of deoxyribosylformamide.

diastereomer mixture was confirmed by the ROESY spectrum (Figure S7, Supporting Information), which contained independent sets of NOESY connectivities (Tables S1 and S8, Supporting Information). By virtue of the NOESY connectivities between H9 and H1′ signals (Figure S7 and Tables S1 and S2, Supporting Information), sugar−base connectivity was established for the two major components **2a** and **2b** of the product mixture, demonstrating the presence of deoxynucleosides rather than a mixture of modified nucleobases and sugars. While only the major components **2a** and **2b** gave detectable NOESY interactions and C/H cross-peaks (vide infra), exchange cross-peaks in the ROESY spectrum permitted **2a** and **2b** to be correlated with the minor components **2a′** and **2b′**, respectively (Figure S7, Supporting Information). On the basis of observation of rotational isomerism around the N8−C9 formamido bond of the 2-Ih base[22] and the formyl C−N bond of *N*-(2′-deoxyribosyl)-formamide,[29,30] rotational isomerism can be ascribed as the exchange mechanism and **2a′** and **2b′** are assigned as the minor rotational isomers around the formamido N8−C9 bond of the respective major nucleoside components. A signal present in the ^{1}H NMR spectrum at 5.72 ppm partially overlaps H1′ assigned to **2a′** (Figures 7 and S7, Supporting Information) and shows NOESY connectivity to a signal overlapping H9 of **2b** at 8.65 ppm. However, this set of signals (indicated by "X" in Figure 7) lacks exchange or NOESY connectivity to any other

(29) Guy, A.; Duplaa, A.-M.; Ulrich, J.; Teoule, R. *Nucleic Acids Res.* **1991**, *19*, 5815–5820.
(30) Maufrais, C.; Fazakerley, G. V.; Cadet, J.; Boulard, Y. *Nucleic Acids Res.* **2003**, *31*, 5930–5940.

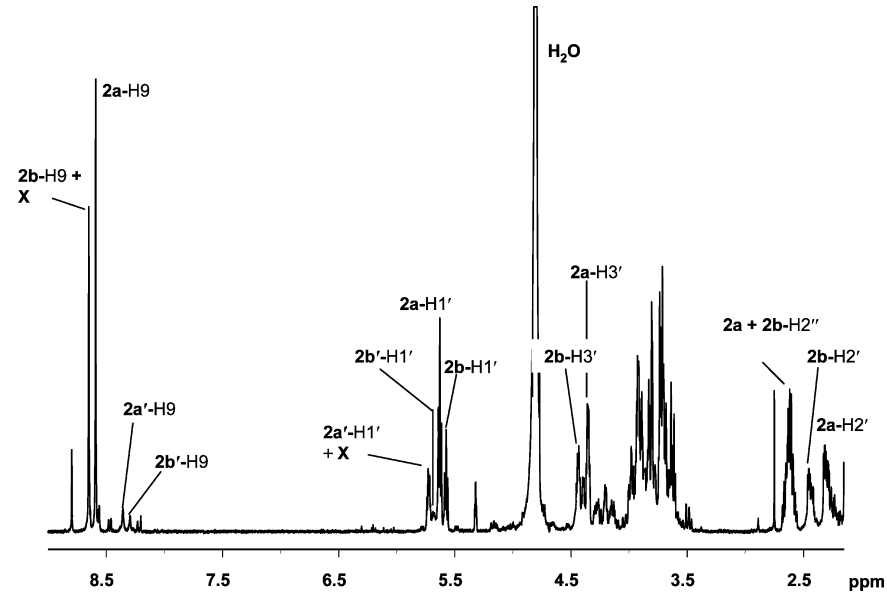

Figure 7. ^{1}H NMR (500 MHz, D_2O) spectrum of the mixture of 2-Ih-dR diastereomers and rotamers **2a**, **2b**, **2a′**, and **2b′** from the oxidation of dGuo by DMDO. For clarity, only well-resolved signals are identified on the trace. An impurity in the H1′ and H9 regions is indicated by "X".

component of the sample and must therefore be an impurity or oxidation side product. To discount the effect of the impurity, the ratio of diastereomers (**2a** + **2a′**)/(**2b** + **2b′**) was estimated from integrated signals of **2a′** and **2b′** in the H9 region and **2a** and **2b** in the H1′ region and found to be ~2/1, while the ratios **2a**/**2a′** (estimated from **2a′**-H9/**2a**-H9) and **2b**/**2b′** (estimated from **1b′**-H1′/**2b**-H1′) are ~10, indicating that a single rotamer is strongly favored for both diastereomers.

Consistent with the ROESY spectrum, the HMBC spectrum of the oxidation mixture (Figure S8, Supporting Information) shows the two independent sets of correlations derived for **2a** and **2b**. The HMBC spectrum of the diastereomer mixture confirms sugar−base connectivities for the major rotational isomers **2a** and **2b** observed in the ROESY spectrum and allows assignment of the deoxyribose carbon shifts as well as the shifts of formyl C9 and spiro C5 of the hydantoin ring. Sugar−base $^3J_{C,H}$ couplings observed for **2a** are between C9 and H1′ and H1′ and C5. Both H1′ and H9 are coupled to a carbon at 76.2 ppm having no attached proton (no C/H cross-peak observed at the corresponding carbon shift in the HSQC spectrum (Figure S9, Supporting Information)) which is therefore assigned to spiro C5 (Table S3, Supporting Information). A carbon shift of 76.2 ppm is within the range of shifts reported for the spiro carbons of the 2-Ih[22] and spiroiminodihydantoin bases and the diastereomeric spiroiminodihydantoin deoxynucleosides.[31,32] A similar set of sugar−base couplings are observed for **2b** (Table S4, Supporting Information). All remaining deoxyribose C/H cross-peaks of **2a** and **2b** could be assigned by a similar analysis of the HMBC and HSQC spectra of the product mixture. The low concentrations of minor rotamers **2a′** and **2b′** precluded observation of C−H coupling in the heteronuclear shift correlation spectra.

Diastereomers **2a** and **2b** could be separated with ~90% efficiency by semipreparative HPLC. The later-eluting product proved to be **2a**. The ROESY spectra of the resolved diastereomers (Figures S10 and S11, Supporting Information) permitted the deoxyribose NOESY connectivities to be identified for the major rotational isomers (Tables S1 and S2, Supporting Information).

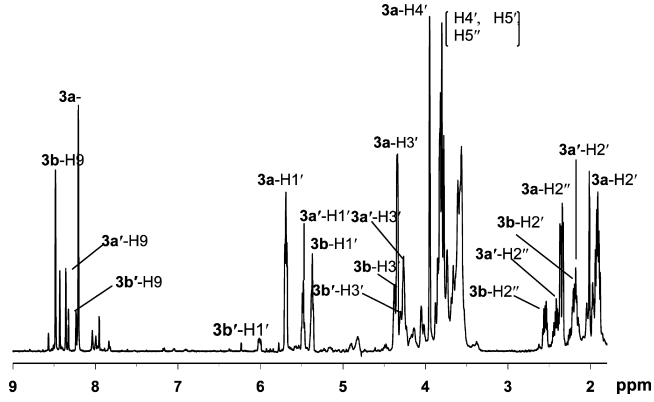

Figure 8. ^{1}H NMR (500 MHz, D_2O) spectrum of a mixture of 2-Ih-dRP diastereomers and rotamers **3a**, **3a′**, **3b**, and **3b′** from the oxidation of dGMP by DMDO. Signal assignments are given on the trace.

Oxidation of dGMP by DMDO. Exact mass measurement of the single molecule ion from the mixture of dGMP oxidation products corresponded in composition to the protonated 2-Ih-dRP dimer (2-Ih-dRP)$_2$H$^+$. The ^{1}H NMR spectrum (Figure 8) is qualitatively similar to that of the mixture of 2-Ih nucleosides and shows two major components **3a** and **3b** along with two minor components, **3a′** and **3b′**. The components of the dGMP oxidation mixture were identified by applying the same strategy described above for the nucleosides. Signals in the H9−H1′ and H2′−H2″ regions were well-resolved. In the ROESY spectrum (Figure S12, Supporting Information), independent sets of NOESY connectivities were determined for **3a** and **3b**, as well as for one of the minor components, which we have assigned as a rotational isomer of **3a′** by virtue of exchange connectivity with **3a** (Tables S5−S7, Supporting Information). An expansion of the H9−H1′ region of the ROESY spectrum (Figure 9) shows exchange connectivity of both minor components **3a′** and **3b′** to corresponding major components **3a** and

(31) Adam, W.; Arnold, M. A.; Grüne, M.; Nau, W. M.; Pischel, U.; Saha-Möller, C. R. *Org. Lett.* **2002**, *4*, 537–540.
(32) Niles, J. C.; Wishnok, J. S.; Tannenbaum, S. R. *Org. Lett.* **2001**, *3*, 963–966.

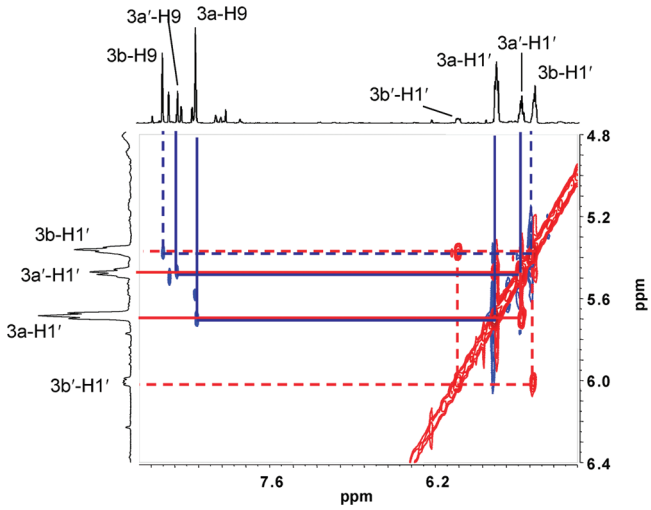

Figure 9. ROESY NMR spectrum of the H1′−H9 region of the mixture of diastereomers and rotamers from the oxidation of dGMP by DMDO. Cross-peaks of signals related by rotational exchange are red. NOESY cross-peaks are blue. Exchange and NOESY connectivities between **3a** and **3a′** are indicated by solid lines and between **3b** and **3b′** by dashed lines.

3b. With the exception of the H5′−H5″ region, where signals of all species in the product mixture overlap, resolution of signals in the ^{1}H NMR and ROESY spectra was sufficient to permit unambiguous assignment of proton signals for three of the four species present. The concentration of **3b′** was too low to allow assignment of signals aside from H1′ and H9. By summing integral ratios in the H1′ region, the ratio (**3a** + **3a′**)/(**3b** + **3b′**) is ∼2/1, in line with the results from dGuo oxidation, while the ratio of rotamers **3a/3a′** is ∼3/1 and **3b/3b′** is >5/1. For **3a**, **3a′**, and **3b**, NOESY cross-peaks between formyl H9 and sugar H1′ signals demonstrate the required connectivity between the base and sugar (Figure 9). In the case of **3b′**, the connectivity between the sugar and base can be inferred from the observation that **3b′** is generated from **3b** by rotational exchange.

For **3a**, **3a′**, and **3b**, assignment of cross-peaks in the heteronuclear shift correlation spectra was determined from the HMBC, HSQC, and ^{13}C spectra (Figures S13−S15, Supporting Information). ^{1}H and ^{13}C assignments derived from these data are given in Tables S8−S10, Supporting Information. The ^{1}H assignments are in complete accord with those derived from the ROESY spectrum. Base−sugar connectivity was confirmed by the three-bond couplings H9−C1′, C9−H1′, and C5−H1′ observed for **3a**, **3a′**, and **3b**. The chemical shifts of the spiro carbons were assigned from the HMBC spectrum on the basis of ^{13}C cross-peaks at shifts of ∼80 ppm with H1′ protons and the absence of signals from carbons in this region of the HSQC spectrum. The assignments of carbon signals to C4′ and C5′ are established by observation of the predicted ^{31}P−^{13}C coupling in the ^{13}C NMR spectrum[33] (Figure S15, Supporting Information). Because of the low concentration of **3b′** in the mixture, only the H1′/C5 cross-peak in the HMBC spectrum could be assigned. Nevertheless, this assignment is important because it unequivocally establishes the sugar−base connectivity of **3b′**.

Oxidation of dGTP by DMDO. Because of the lability of the phosphates in dGTP, the oxidation mixture was maintained at 0 °C and the product **4** characterized in the total reaction mixture without further purification being attempted. The major ions in the negative ion ESI-MS spectrum corresponded to mono- and disodium adducts of the deprotonated molecule $[M - H]^-$, $[MNa - H]^-$ and $[MNa_2 - H]^-$, along with product ions $[M - H_2PO_3]^-$ and $[MNa - HP_2O_7]^-$. The ^{1}H NMR spectrum of the crude reaction mixture (Figures S16, Supporting Information) was qualitatively similar to those of the product mixtures from oxidation of dGuo and dGMP. In the HMBC spectrum (Figures S17, Supporting Information), one set of connectivities could be unambiguously ascribed to one 2-Ih-dRTP diastereomer. A component of a multiplet at ∼5.75 ppm in the H1′ region couples with a carbon resonance at 164.0 ppm which can be assigned to C9 of the 2-Ih base by virtue of unsuppressed one-bond coupling to a formyl H9 signal at 8.43 ppm. The H1′ and formyl H9 signals both couple to a carbon at 78.3 ppm having no attached proton and identified on this basis as spiro C5 of the 2-Ih base. The formyl H9 also couples to a carbon signal in the C1′ region at 88.4 ppm which in turn couples to a proton in the H2′ region at 2.11 ppm. Two additional products in the HMBC spectrum have signals within the H9 region of 2-Ih which show unsuppressed one-bond coupling to carbons at shifts consistent with 2-Ih formyl C9 and also coupling to carbons in the 2-Ih spiro C5 region. However, connectivity between the base moieties and a sugar cannot be definitively established for these components from the HMBC data.

Discussion

Oxidation of DNA. Of paramount interest was whether peracids and DMDO would transform guanine to 2-Ih in single- and double-stranded DNA. We approached this question by DMDO oxidation of the 5-mer d(TTGTT) and the short duplex d[(TTGTT)·(AACAA)]. The single-stranded 5-mer d(TTGTT) treated with a ∼7-fold excess of DMDO was 95% oxidized, with at least 40% conversion to 2-Ih-modified oligonucleotides estimated from ^{1}H NMR analysis on the basis of integration of signals identified as H1′ and H9. The negative ion MALDI-TOF MS spectrum of the crude oxidation mixture showed a strong ion at *m*/*z* 1516, a gain of 34 mass units relative to the deprotonated molecular ion of the unmodified sequence and consistent with formation of the 2-Ih lesion. Fragmentation of this ion, observed by ESI-MS/MS, provided further support for the oxidation of Gua to 2-Ih, showing a collision-induced fragmentation pattern consistent with breaking of the C5−N8 bond to yield ions of the oligonucleotide containing the deoxyribosyl formamide group in both positive and negative ion modes (Figures S3 and S5, Supporting Information). The HPLC trace of the reaction mixture indicates a single major product, having an ESI-MS spectrum consistent with that of the 2-Ih-modified 5-mer. 2-Ih in the oxidized 5-mer was definitively confirmed by digestion and identification of 2-Ih-dR in the mixture of mononucleosides.

Oxidation of d[(TTGTT)·(AACAA)] also resulted in generation of 2-Ih, unequivocally identified as the deoxynucleoside by the retention time in HPLC analysis of the digest and by positive ion ESI-MS/MS of the ion corresponding to $[MH]^+$ (Figures S16, Supporting Information). Significantly, the 2-Ih lesion is sufficiently stable to withstand both digestion and chromatographic separation. This observation and the stability of the glycosidic bond under acid conditions as evident from the isolation of 2-Ih nucleoside from *m*-CPBA oxidation of dGuo indicate that 2-Ih, if formed in vivo, might be expected to persist as a stable lesion. Oxidation of DNA by *m*-CPBA has been reported to target purines, particularly in loop regions, with generation of blocking lesions.[23] The lesions were not structur-

(33) Niemczura, W. P.; Hruska, R. E. *Can. J. Chem.* **1980**, *58*, 472–478.

ally characterized at the time, but our determination that 2-Ih is a product of Gua oxidation in DNA by *m*-CPBA suggests that 2-Ih may in part account for the reported interference of the oxidative lesions with replication.

Gua + 34 species have been reported from the oxidation of Gua in DNA by a manganese porphyrin/$KHSO_5$ system, which can function as a monooxygen transfer catalyst,[34] and by a dicopper−phenolate complex, via a putative hydroperoxodicopper(II) transient.[35] A possible mechanism for the formation of this product with the manganese porphyrin catalyst was proposed by the authors[10] which involves the trapping of water by a transient guanine cation and formation of **5** followed by hydrolytic opening of the imidazolone ring by breaking the bond between the imino carbon and the nitrogen attached to the deoxyribose to give an *N*-formylamido-substituted structure rather than the *N*-formylamino-substituted structure of our Scheme 1. However, the assignment of the *N*-formylcarboxamido structure was speculative, while we have rigorously established the *N*-formylamino substitution of 2-Ih by a combination of labeling and NMR studies discussed below. We therefore suggest the *N*-formylamino structure of 2-Ih as a plausible alternative for the products reported in refs 10 and 34.

Oxidation of dGuo by Peracids. Peracetic acid is representative of low molecular weight alkyl peracids that might be generated in biological processes[14−18] and is also a convenient model oxidant because the acetic acid byproduct of oxidation can be removed from reaction mixtures under vacuum, avoiding the need for chromatographic separation of products from spent oxidant. A drawback of aqueous peracetic acid is the presence of hydrogen peroxide as a ∼6% equilibrium component,[36] raising the possibility of concurrent oxidation via the Fenton reaction catalyzed by trace transition metals[37] and/or radical pathways. Thus, the Sp and Sp-dR which have been reported as products of dGuo oxidation by Fenton chemistry[37] and other one-electron pathways[38,39] can most likely be attributed to alternative pathways as a result of the hydrogen peroxide in peracetic acid. Deglycosylation of the 2-Ih and Sp nucleosides evident in Figure 4a is not surprising in view of the lengthy reaction time at pH < 4 required to maintain peracetic acid in the active, protonated form. The choice of *m*-CPBA as a peracid oxidant rested on the availability in our laboratory of [$^{18}O_2$]-*m*-CPBA with an ^{18}O content >95%, allowing us to determine the number and site of oxygen atoms incorporated from the peracid. The *m*-CPBA oxidation yielded 2-Ih-dR and a minor amount of the aglycon as virtually exclusive oxidation products (Figure 4b), supporting the suggestion that Sp observed in the oxidation of Gua with peracetic acid was a consequence of the equilibrium concentration of hydrogen peroxide. Only trace quantities of Sp-dR and its aglycon were detected in the *m*-CPBA oxidation, possibly products of a minor radical pathway via O−O homolysis of *m*-CPBA.[40,41] The product profile generated by *m*-CPBA oxidation strongly supports 2-Ih as the product of the peracid oxidation of dGuo in protic solvents, and the predominance of the nucleoside as a product at pH 4.5 indicates that the glycosidic bond is robust and should be stable under physiological conditions.

Labeling Studies and Oxidation Mechanism. We have proposed Scheme 1 as the mechanism for the oxidation of guanine to 2-Ih by epoxidizing agents, supported by the oxidation of [4-^{13}C]- and [7-^{15}N]guanine by DMDO.[22] As required by the 1,2-carbonyl shift, the ^{13}C label at position 4 of guanine becomes spiro carbon C5 of 2-iminohydantoin. Also in accord with Scheme 1, oxidation of [7-^{15}N]guanine yielded 2-Ih with ^{15}N label at the carboxamido nitrogen. Hydrolytic opening of the transient imidazolone ring via **5** is then predicted to give 2-Ih. Ring cleavage of **5** to 2-Ih according to Scheme 1 has been definitively established by the presence of two inequivalent carboxamido NH signals in the ^1H NMR spectrum of 2-Ih, which show $^1J_{N-H}$ coupling of ∼90 Hz in the 7-^{15}N isotopomer.[22] These observations rule out an *N*-formylamido structure which, as discussed above, has been proposed to result from the hydrolytic ring-opening of transient **5** in the manganese porphyrin-catalyzed persulfate oxidation of Gua in DNA.[10] The ^{18}O incorporation studies, which show that the carboxamide oxygen is derived from oxidant and the formamide oxygen from water, rule out the intermediacy of 8-oxo-dGuo in formation of 2-Ih. The ^{18}O labeling pattern precludes formation of an 8-oxo-dGuo transient via direct oxygen donation by *m*-CPBA but is consistent with trapping of water by a radical or radical cation formed via initial electron abstraction followed by a second one-electron oxidation, as has been proposed earlier [Scheme 12, ref 10]. The further oxidation of 8-oxo-dGuo with the requirement that the peracid be the source of the carboxamido oxygen necessitates oxidation at C5 with oxygen transfer by *m*-CPBA, accompanied by a 1,2-acyl shift of C6. Such a transformation could be accomplished either by epoxidation of the C4−C5 bond or by a Baeyer−Villiger-like oxidation at C6 followed by ring contraction. However, the product would in either case be Sp, and hydrolytic opening of the hydantoin ring without a reducing step would yield a carbamic acid rather than an *N*-formyl product. A major argument against the reaction pathways involving the intermediacy of 8-oxo-Gua formed by initial electron abstraction is that they require the consumption of four oxidizing equivalents, which is inconsistent with the 79% yield of 2-iminohydantoin obtained using one molar equivalent of *m*-CPBA. Initial electron abstraction from guanine, which has a higher oxidation potential, rather than from a subsequent 8-oxo-dGuo transient, and a reductive cleavage of the hydantoin ring are also difficult to rationalize. The ^{18}O-labeling experiments thus support Scheme 1 as the predominant oxidation pathway by peracids and DMDO and also support the high level of conversion of Gua to 2-Ih in the oxidation of DNA, as implied by the analysis of the oxidized single- and double-stranded oligonucleotides. The oxidation of Gua at the C4−C5 bond without oxidation at C8 in Scheme 1 is consistent with recent reports of selective oxidation at C5 of Gua in the formation of a cross-link between Gua and Lys,[11] and also in the reaction sequence following attack of hydroxyl radical at C5′ of dGuo.[42]

(34) Vialas, C.; Claparols, C.; Pratviel, G.; Meunier, B. *J. Am. Chem. Soc.* **2000**, *122*, 2157–2167.
(35) Li, L.; Karlin, K. D.; Rokita, S. E. *J. Am. Chem. Soc.* **2005**, *127*, 520–521.
(36) Dul'neva, L. V.; Moskvin, A. V. *Russ. J. Gen. Chem.* **2005**, *75*, 1125–1130.
(37) White, B.; Tarun, M. C.; Gathergood, N.; Rusling, J. F.; Smyth, M. R. *Mol. BioSyst.* **2005**, *1*, 373–381.
(38) Luo, W.; Muller, J. G.; Rachlin, E. M.; Burrows, C. J. *Org. Lett.* **2000**, *2*, 613–616.
(39) Cadet, J.; Douki, T.; Gasparutto, D.; Ravanat, J.-L. *Mutat. Res.* **2003**, *531*, 5–23.
(40) Ryu, E. K.; MacCoss, M. *J. Org. Chem.* **1981**, *46*, 2819–2823.
(41) Bravo, A.; Bjorsvik, H.-R.; Fontana, F.; Minisci, F.; Serri, A. *J. Org. Chem.* **1996**, *61*, 9409–9416.
(42) Boussicault, F.; Kaloudis, P.; Caminal, C.; Mulazzani, Q. G.; Chatgilialoglu, C. *J. Am. Chem. Soc.* **2008**, *130*, 8377–8385.

Structural Analysis of the DMDO Oxidation of dGuo, dGMP, and dGTP. Oxidations with DMDO as oxidant were carried out on a scale permitting rigorous structural characterization of the product profiles. The presence of the N9 sugar substituent would be expected to generate resolvable diastereomers resulting from enantioselective induction of the asymmetric center at spiro C5. The DMDO oxidations of dGuo and dGMP conform to expectation; both starting compounds yield two diastereomers in a ~2/1 mixture. In addition, slow rotation around the N8−C9 formamido bond resulted in resolution of two rotational isomers for each diastereomer, analogous to behavior reported for the 2-Ih base[22] and the *N*-(2′-deoxyribosyl)formamide lesion.[29,30] The major rotational isomers of the 2-Ih diastereomers at the deoxynucleoside level were favored by an order of magnitude over the minor rotamers. Rotamer preference was less pronounced for the deoxynucleotide diastereomers, with ratios being 3/1 for the major diastereomer **3a** and ~5/1 for the minor diastereomer **3b**.

5. Conclusion

The oxidation of guanine to 2-Ih was shown to be a major transformation in the oxidation of the single-stranded DNA 5-mer d(TTGTT) with *m*-CPBA and DMDO as a model for peracid oxidants and in the oxidation of the 5-base pair duplex d[(TTGTT)·(AACAA)] with DMDO. 2-Ih has not previously been reported as an oxidative lesion in DNA. This study supports the identification of previously incompletely characterized DNA lesions with molecular weights of Gua + 34 induced by transition-metal complexes[10,34,35] as 2-Ih. Rigorous structural characterization and mechanistic studies with incorporation of stable isotopes unambiguously established the structure of the 2-Ih-dR formed from dGuo by peracetic acid, *m*-CPBA, and DMDO. The corresponding nucleotides are also generated from dGMP and dGTP by DMDO. The reaction proceeds by initial epoxidation of the C4−C5 bond of Gua followed by a 1,2-shift of Gua C6 to give a dehydrodeoxyiminodihydantoin and subsequent hydrolytic opening of the imidazolone ring to give 2-Ih, confirmed by the demonstration that the carbonyl oxygen at C6 of 2-Ih is derived from the oxidant and the formyl oxygen at C9 from water. Molecular oxygen is not directly required. An important observation consistent with this pathway is that 8-oxo-Gua is not generated as an oxidation product. Damage to DNA by *m*-CPBA was previously shown to block the action of polymerases at purines,[23] suggesting that the 2-Ih lesion has potential to interfere with DNA replication, in addition to serving as a marker for biological oxidation via 2-electron pathways that do not produce 8-oxo-Gua, and would therefore not be accounted for by current assays for biomarkers of oxidative stress.

Acknowledgment. This work was supported in part by PHS Grant P42-ES005948 and NIEHS Contract ESR30262. K.B.T. and J.W. thank the Intramural Research Program of the NIEHS/NIH (Grant Z01 ES050171) for support. The UNC-Duke Proteomics Center was partially funded by a gift from an anonymous donor in honor of Michael Hooker.

Supporting Information Available: Figures S1−S17 and Tables S1−S10 giving the complete heteronuclear shift correlation spectra, mass spectra for characterization of 2-Ih nucleoside, nucleotide, and nucleoside triphosphates, mass spectra of ^{18}O label incorporation, and tabulated NOESY and C/H cross-peaks. This material is available free of charge via the Internet at http://pubs.acs.org.

JA8090752